ADVANCED MATERIALS
www.advmat.de

Synthesis of Diimidazolylstilbenes as n-Type Blue Fluorophores: Alternative Dopant Materials for Highly Efficient Electroluminescent Devices

*Ho-Hsiu Chou, Yi-Hsiang Chen, He-Pei Hsu, Wen-Hsin Chang, Yu-Han Chen, and Chien-Hong Cheng**

Organic light-emitting diodes (OLEDs) have attracted great attention due to their application in high-resolution, full-color, flat-panel displays and lighting sources.[1] The search for stable and highly efficient emitters for the three primary colors is crucial for OLEDs to be useful commercially.[2] Recently, the development of red and green electrophosphorescent devices with high efficiencies, long lifetimes, and pure color Commission International de l'Eclairage (CIE) co-ordination has been achieved. However, it is much more difficult to find a blue phosphorescent emission with long lifetime and pure color CIE, due to the inherent wide bandgap. Thus, although many blue phosphorescent devices can achieve high external quantum efficiencies (EQEs),[3,4] high CIE co-ordinates (y co-ordinate ≥ 0.25) and/or short device lifetimes are not suitable for them to be commercially used. Therefore, in order to achieve marketable OLEDs, the hunt for highly efficient blue-fluorescent materials and devices is still a subject of current interest.

For a blue-fluorescent device, it is well known that the device efficiency, color co-ordinates, and operational stability can be significantly improved by using a doped emitter.[5,6] To date, many blue-fluorescent dopant materials containing p-type moieties such as arylamino or carbazolyl have been reported. The distyrylarylene (DSA) amines, 4,4′-bis((E)-2-(9-ethyl-9H-carbazol-3-yl)vinyl)-1,1′-biphenyl (BCzVBi)[7] and 4,4′- 4,4′-bis[2-(4-(*N*,*N*-diphenylamino)phenyl)vinyl]biphenyl (DPAVBi),[8] were first reported by Hosokawa et al. and were widely used as the blue dopants for electroluminescent devices.[7–9] A mono(styryl) amine (*E*)-4-(2-([1,1′:4′,1′′-terphenyl]-4-yl)vinyl)-*N*,*N*-diphenylaniline (BD1)-based device showing a current efficiency of 5.4 cd A^{-1} and an external quantum efficiency of 5.1%, with CIE co-ordinates of (0.14, 0.13), was demonstrated by Chen and coworkers.[1c] Jin and coworkers. reported blue-fluorescent devices using BCzVBi as the dopant, with a current efficiency of 6.9 cd A^{-1} at CIE co-ordinates of (0.155, 0.157).[10] A series of spiro styrylamines were synthesized and used as blue dopants by Lee et al. and Yoon and coworkers.[11] One of the doped devices showed a high current efficiency of 9.11 cd A^{-1} with CIE co-ordinates of (0.14, 0.16). We recently also used BCzVBi as the dopant and phenanthrene derivatives as hosts to achieve a current efficiency as high as 9.8 cd A^{-1} at CIE co-ordinates of (0.14, 0.14).[12] In addition, several reports using p-type molecules containing the styrylamine moiety as the blue fluorescent dopant are also known.[1c,6–8,13]

Unlike p-type blue-fluorescent dopant materials, blue-fluorescent dopant materials with n-type moieties are relatively rare. The n-type imidazole moiety, has been widely employed as an electron-transporting material[14] and as the electron-withdrawing group of bipolar host materials.[15] We have shown that [1,4-bis(2-(4-benzoylphenyl)-5-phenyl-1*H*-4-imidazolyl) benzene] is an n-type blue dopant emitter for electroluminescent devices, achieving CIE co-ordinates of (0.15, 0.12), although the device efficiencies are low.[16] The n-type spirobifluorene-based pyrazoloquinoline dopant materials developed by Shu and coworkers showed a current efficiency of 4.5 cd A^{-1} with CIE co-ordinates of (0.14, 0.17) for one of the corresponding devices.[17] Recently, the synthesis of phenanthroimidazolyl derivatives and the application of these materials as the host emitters for nondoped devices were reported by our group.[18a] In addition, Ma and coworkers further demonstrated that the phenanthroimidazolyl unit is an excellent electron-injection structure.[14c] In this paper, we report the synthesis of two new imidazole derivatives (*E*)-1,2-bis(4-(1-phenyl-1*H*-phenanthro[9,10-*d*]imidazol-2-yl)phenyl) ethene (PPIE) and (*E*)-1,2-bis(4-(1,4,5-triphenyl-1*H*-imidazol-2-yl)phenyl)ethene (TPIE) and the application of these two molecules as extremely high efficiency blue-fluorescent dopants for electroluminescent devices.

Both PPIE and TPIE adopt a stilbene group as the core structure end-capped with two 1-phenyl-1*H*-phenanthro[9,10-d]imidazol-2-yl and 1,4,5-triphenyl-1*H*-imidazol-2-yl groups, respectively. They were synthesized in one pot from the corresponding dialdehyde and dione derivatives in the presence of aniline, ammonium acetate, and acetic acid (**Scheme 1**).[18] The crystal structures of PPIE and TPIE were determined using single-crystal X-ray diffraction (Supporting Information, Figure S1 and S2).[19] In both crystal structures, the central stilbene group adopts a planar structure, but the stilbene and imidazole planes are no longer coplanar, showing dihedral angles of 41° and 37°, respectively. Similarly, in both compounds, the *N*-phenyl and the imidazole planes intersect with dihedral angles of ca. 68°. On the other hand, the 1*H*-phenanthro[9,10-*d*]imidazole group in PPIE is planar, but in TPIE the imidazole moiety and the two phenyl moieties attached reveal dihedral angles of 28° and 46°, respectively. This structural difference between PPIE and TPIE is expected to alter the highest occupied molecular orbital (HOMO) and lowest unoccupied

Dr. H.-H. Chou, Y.-H. Chen, H.-P. Hsu,
W.-H. Chang, Y.-H. Chen, Prof. C.-H. Cheng
Department of Chemistry
National Tsing Hua University
Hsinchu 30013, Taiwan
E-mail: chcheng@mx.nthu.edu.tw

DOI: 10.1002/adma.201202222

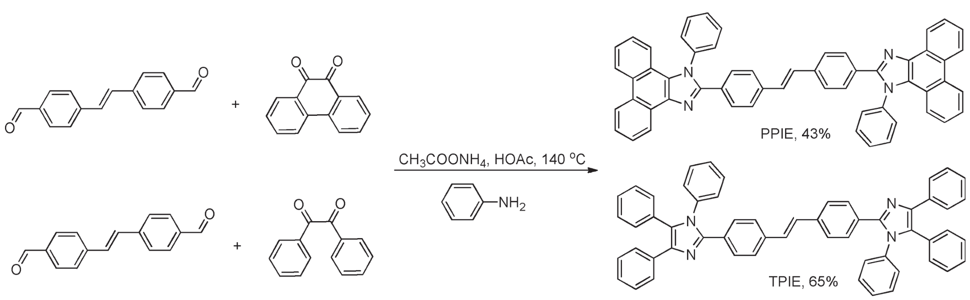

Scheme 1. The synthesis route of PPIE and TPIE.

molecular orbital (LUMO) energy levels, as well as the thermal and photoluminance properties. The ^{1}H and ^{13}C NMR spectra, mass spectral data, and elemental analysis are in agreement with the structures determined by X-ray-diffraction analysis.

The absorption and photoluminescence (PL) spectra of PPIE and TPIE are shown in **Figure 1**, while the peak maxima of these spectra are summarized in **Table 1**. The absorption spectra of these two compounds appear simple, showing only one band at 387 and 373 nm for PPIE and TPIE, respectively. There are two emission maxima in the blue region for each of these two compounds. As expected, the emission maxima of PPIE in tetrahydrofuran (THF) solution at 444 and 469 nm are slightly red-shifted compared with those of TPIE at 432 and 452 nm. The emission spectra of PPIE and TPIE doped in 1-(2,5-dimethyl-4-(1-pyrenyl) phenyl)pyrene (DMPPP)[20] thin films via vacuum deposition with a concentration of 5% and thickness of 25 nm on a quartz plate were also measured. These emission peaks in DMPPP are red-shifted by ca. 10 nm relative to the corresponding peaks in THF. In the neat thin film, the PL spectra are further red-shifted by 41 nm for PPIE and by 26 nm for TPIE (Figure S3). The large red shift of the PPIE neat film is probably due to the presence of the planar phenanthroimidazolyl ring that facilitates stronger π–π stacking. Both PPIE and TPIE show very high PL quantum yields (QYs) of 0.83 and 0.80, respectively, in dilute cyclohexane solution. The values were measured by using 9,10-diphenylanthrecene (QY = 0.90 in cyclohexane) as in work by Li et al.[21] In addition, we also measured the solid-state photoluminescence QY of PPIE and TPIE doped in DMPPP thin films (50 nm) with a concentration of 2%. Both PPIE and TPIE exhibited excellent QYs of 0.92 and 0.83, respectively, and were higher than the QY of DPAVBi (QY = 0.80) and BCzVBi (QY = 0.83) measured also in the DMPPP film under the same conditions.

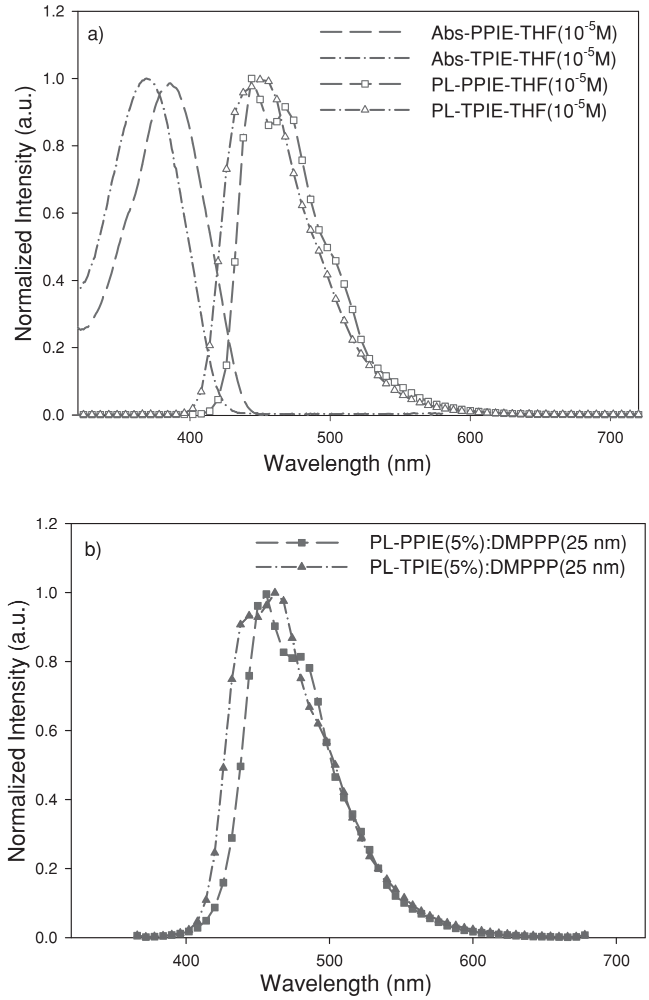

Figure 1. a) Normalized absorption and PL spectra of PPIE and TPIE in THF (1 × 10^{-5} M). b) Normalized PL spectra of PPIE- and TPIE-doped DMPPP films (25 nm) at a dopant concentration of 5%.

The molecular orbital levels of these two compounds were determined by photoelectron spectrometry and UV–vis absorption measurements. The HOMO levels of PPIE and TPIE appeared at 5.35 and 5.47 eV, respectively. The LUMO levels, both appearing at 2.66 eV, were calculated by subtracting the energy gap from their HOMO levels. The HOMO level of PPIE was higher than that of TPIE due to the extended π-conjugation of the fused phenanthroimidazolyl structure. To gain insight into the electronic states of these two compounds, density functionalized theory (DFT) calculations were performed (Figure S4). The results show that the LUMO of PPIE and TPIE are localized on the stilbene and imidazole moieties. However, the HOMO of PPIE is further extended to the phenanthrene moiety, while the HOMO of TPIE is extended to the two phenyl groups at the 4,5-position of imidazole. The observations are in a good agreement with the fact that PPIE and TPIE have the same LUMO levels but different HOMO levels. Moreover, the involvement of the imidazole group in the LUMO's of both PPIE and TPIE suggests that they can be considered as n-type materials.[14,15]

DOI: 10.1002/adma.201202222

Table 1. The photophysical and thermal properties of PPIE and TPIE.

Compound	λ_{abs}a) [nm]	λ_{fl}a) [nm]	λ_{fl}b) [nm]	E_gc) [eV]	HOMOd) [eV]	LUMOe) [eV]	$T_g/T_m/T_d$ [°C]	QYf)
PPIE	387	444, 469	454, 478	2.69	5.35	2.66	190/401/497	0.83 (0.92)
TPIE	373	432, 452	442, 464	2.81	5.47	2.66	151/358/459	0.80 (0.84)

a)The absorption and fluorescence spectra were measured in THF solution at concentration = 1 × 10^{-5} M; b)The fluorescence spectra were measured in the PPIE- or TPIE-doped DMPPP film (25 nm); c)Estimated from the thin-film optical-absorption threshold; d)Estimated by photoelectron spectrometry (AC-II); e)LUMO = HOMO – E_g; f)The quantum yield was measured in cyclohexane using 9,10-diphenylanthrecene (QY = 0.90) as the standard; the data presented in parentheses are the solid-state photoluminescent quantum yields of the dopants in DMPPP thin film.

To find further support for the electron-transporting character of diimidazolylstilbenes, two electron-only devices were fabricated. The devices consist of the following structure: indium tin oxide (ITO)/BCP (15 nm)/dopant (30 nm)/BCP (15 nm)/LiF (1 nm)/Al (100 nm), where the dopant is either PPIE or TPIE and BCP is 2,9-dimethyl-4,7-diphenyl-1,10-phenanthroline. We also fabricated a similar electron-only device using DPAVBi as the dopant for comparison. In these devices, BCP layers were used to prevent hole injection from the anode. The current density versus voltage curves of these three devices (Figure S5) show that the TPIE- and PPIE-based electron-only devices gave a higher current density than the DPAVBi-based one. The observations strongly support that both PPIE and TPIE are n-type materials capable of transporting electrons.

The thermal properties of PPIE and TPIE were determined by differential scanning calorimetry (DSC) and thermogravimetric analysis (TGA). The resultant data including melting point (T_m), glass-transition temperature (T_g), and decomposition temperature (T_d) are shown in Table 1 and Figure S6. Among these two diimidazolylstilbenes, the decomposition temperatures are in the order PPIE > TPIE. In addition, the DSC results show that PPIE with two fused phenanthroimidazolyl structures possesses a higher thermal stability. After rapid cooling from the melt state followed by a slow warm up, PPIE shows two endothermic transitions at 190 and 401 °C, corresponding to the T_g and T_m, and one exothermic transition at 255 °C, corresponding to the crystallization temperature (T_c). For TPIE, the T_g appears at 151 °C and T_m at 376 °C, whilst no T_c was observed. To examine the thermal morphological stability further, we used atomic force microscopy (AFM) to measure the topography of PPIE and TPIE thin films at room temperature and at 90 °C for 18 h. The root-mean-square roughness (R_{rms}) of these thin-film surfaces showed no substantial changes before and after annealing (90 °C) (Figure S7). The results of the thermal-property studies reveal that PPIE and TPIE have very high glass-transition temperatures and melting points, and that the morphology of their thin films show high thermal stability.

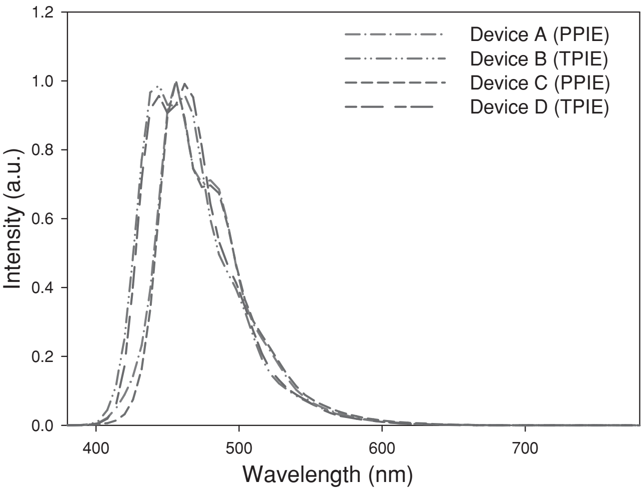

Figure 2. EL spectra for devices A–D at 8 V.

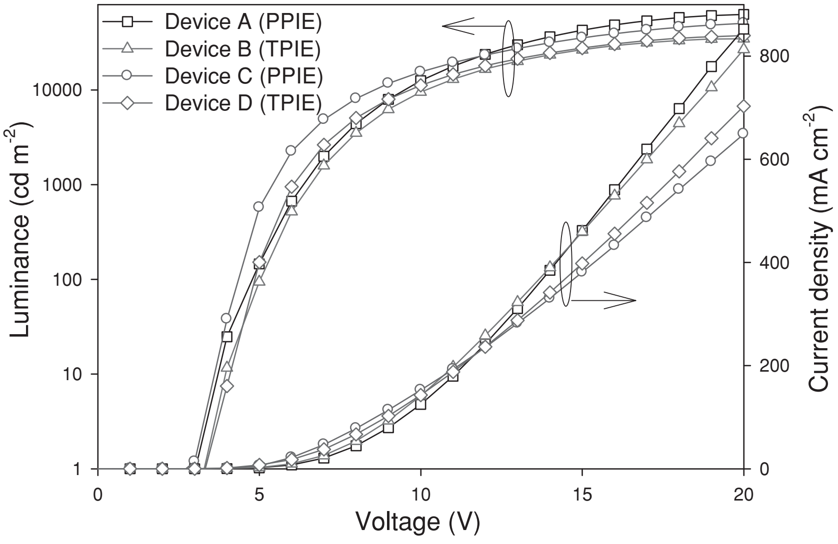

Figure 3. Luminance and current density versus voltage for devices A–D.

To know the suitability of these n-type diimidazolylstilbenes as the electroluminescent (EL) materials, we fabricated devices A–D by utilizing PPIE and TPIE as the dopants and DMPPP as the host (Figure S8). The EL spectra, luminance and current density vs. applied voltage, and EQE and current efficiency vs. luminance of these devices are displayed in **Figure 2–4**. Devices A and B consist of the layers: NPNPB (50 nm)/NPB (10 nm)/DMPPP: PPIE or TPIE (5%) (25 nm)/BAlq (20 nm)/

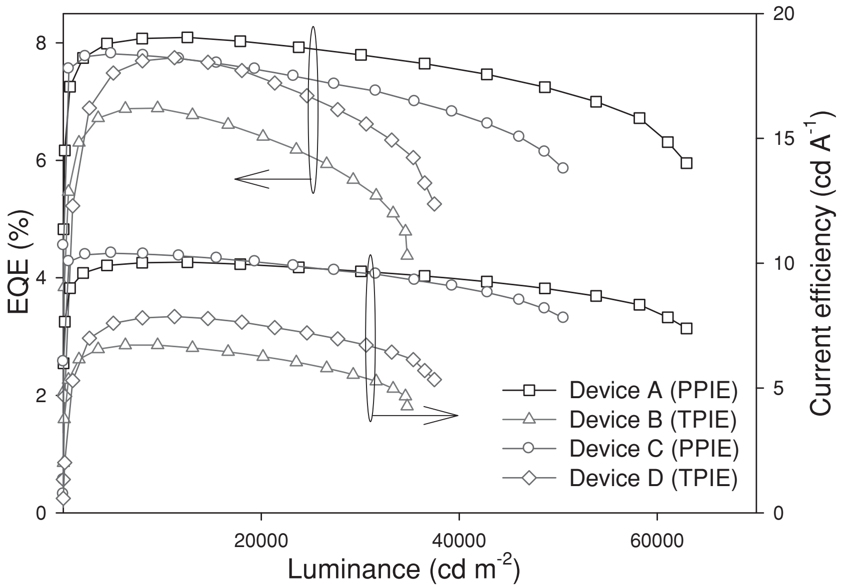

Figure 4. EQE and current efficiency versus luminance for devices A–D.

LiF (1 nm)/Al (100 nm), where NPNPB = *N,N′*-diphenyl-*N,N′*-di-[4-(*N,N*-diphenyl-amino)phenyl]benzidine, NPB = *N,N′*-di(1-naphthyl)-*N,N′*-diphenyl-(1,1′-biphenyl)-4,4′-diamine, and BAlq = bis(2-methyl-8-quinolinolate)-4-(phenylphenolato) aluminum. Devices A and B exhibited high EQEs of 8.1 and 6.9%, current efficiencies of 10.0 and 6.8 cd A^{-1}, and CIE co-ordinates of (0.14, 0.14) and (0.15, 0.10), respectively. The performance of PPIE and TPIE-based devices can be improved by inserting a thin layer of 4,4′,4″-tri(9-carbazoyl)triphenylamine (TCTA) (10 nm) between NPB and the emitting layer (see **Table 2**). Devices C and D thus fabricated emit deep-blue light with CIE co-ordinates of (0.14, 0.15) and (0.15, 0.11) very efficiently. Extremely high EQEs of 7.8 and 7.7% and current efficiencies of 10.4 and 7.9 cd A^{-1}, respectively, were observed. In particular, the PPIE-based device C showed a low turn-on voltage of 2.8 eV with an excellent power efficiency of 6.4 lm W^{-1}. As shown in Figure 4 and Figure S9, the EQE, current efficiency and power efficiency vs. luminance curves showed very low efficiency roll-off for all of the devices. Interestingly, the EL spectra of devices A–D and the PL spectra of PPIE and TPIE doped in DMPPP thin films are nearly the same. We also used the common p-type deep-blue dopant BCzVBi to fabricate device E with the same configuration (see Table 2 and Figure S10). The performance of device E showed an EQE of 5.7%, a current efficiency of 7.1 cd A^{-1}, and CIE co-ordinates of (0.14, 0.14). The result demonstrates that our n-type dopants have a higher device efficiency than the p-type one. In addition, compared with the performance of previously reported blue-fluorescent devices with true blue CIE co-ordinates, the extremely high efficiencies of these PPIE- and TPIE-based devices appear to be among the highest reported to the best of our knowledge.

Table 2. Performances of devices A, B, C, and D.

Device[a]	Dopant	V_{on}	L_{max}[b] [cd m^{-2}]	η_{ext}[c] [%]	η_c[d] [cd A^{-1}]	η_p[e] [lm W^{-1}]	CIE[f] [*x*, *y*]
A	PPIE	3.0	62 956 (20.0 V)	8.1	10.0	4.8	(0.14, 0.14)
B	TPIE	3.1	34 846 (19.5 V)	6.9	6.8	2.8	(0.15, 0.10)
C	PPIE	2.8	50 560 (20.0 V)	7.8	10.4	6.4	(0.14, 0.15)
D	TPIE	3.2	37 484 (20.0 V)	7.7	7.9	3.1	(0.15, 0.11)
E	BCzVBi	3.5	40 894 (18.0 V)	5.7	7.1	3.4	(0.14, 0.14)

[a] The cathode of the general device is LiF (1 nm)/Al (100 nm); the structure of devices A and B: ITO/NPNPB (50)/NPB (10)/DMPPP: Dopant (5%) (25)/BAlq (20); devices C, D and E: ITO/NPNPB (50)/NPB (10)/TCTA (10)/DMPPP: Dopant (5%) (25)/BAlq (20); the unit of thickness is nm; [b] The maximum values of luminance (L_{max}); [c] The external quantum efficiency (η_{ext}); [d] The current efficiency (η_c); [e] The power efficiency (η_p); [f] Taken at 8 V.

In summary, we have demonstrated in this work the use of blue-fluorescent dopants PPIE and TPIE containing the n-type imidazole moiety for EL devices. These two dopants exhibited very high fluorescence quantum yields and thermal stability. The PPIE- and TPIE-based EL devices can achieve excellent EQE (current efficiency) of 7.8% (10.4 cd A^{-1}) and 7.7% (7.9 cd A^{-1}) with true blue CIE co-ordinates of (0.14, 0.15) and (0.15, 0.11), respectively. These n-type materials provide an alternative for dopant emitters in OLEDs other than the well-known p-type ones.

Experimental Section

Procedure for the Synthesis of (E)-1,2-bis(4-(1-phenyl-1H-phenanthro[9,10-d]imidazol-2-yl)phenyl)ethene (PPIE): A mixture of 9,10-phenanthrenequinone (1.06 g, 5.08 mmol), (*E*)-4,4′-(ethene-1,2-diyl)dibenzaldehyde (500 mg, 2.12 mmol), aniline (0.46 mL, 5.08 mmol) and ammonium acetate (3.26 g, 42.3 mmol) in glacial acetic acid (28 ml) was heated at 140 °C under a nitrogen atmosphere for 48 h. After cooling to room temperature, the reaction mixture was poured into a methanol solution with stirring. The separated solid was filtered off, washed with methanol, and dried to give the expected product. The product was sublimed at 370 °C (1×10^{-5} Torr) to give the desired final product in a 43% yield. ^{1}H NMR (500 MHz, $CDCl_3$, δ): 8.86 (d, *J* = 6.5 Hz, 2H), 8.76 (d, *J* = 8.0 Hz, 2H), 8.70 (d, *J* = 8 Hz, 2H), 7.73 (s, 2H), 7.63–7.49 (m, 16H), 7.45 (s, 2H), 7.40 (d, *J* = 9 Hz, 4H), 7.18 (s, 4H), 7.05 (s, 2H); HRMS (M$^+$): calcd for $C_{56}H_{36}N_4$, 764.2940; found, 764.2947. Anal. calcd. for $C_{56}H_{36}N_4$: C 87.93, H 4.74, N 7.32; found, C 87.44, H 4.83, N 7.29.

Similar procedures were used to prepare TPIE from the corresponding aldehyde derivatives. The yields and spectral data are shown below.

(E)-1,2-bis(4-(1,4,5-triphenyl-1H-imidazol-2-yl)phenyl)ethene (TPIE): The product was sublimed at 330 °C (1×10^{-5} Torr) to give the desired final product in a 65% yield. ^{1}H NMR (400 MHz, CD_2Cl_2, δ): 7.58–7.55 (m, 4H), 7.44–7.38 (m, 10H), 7.34–7.16 (m, 20H), 7.13–7.11 (m, 4H), 7.07 (s, 2H); ^{13}C NMR (125 MHz, $CDCl_3$, δ): 146.2, 137.5, 131.1, 131.0, 129.3, 128.7, 128.4, 128.3, 128.3, 127.6, 127.1, 126.4. HRMS (M$^+$): calcd for $C_{56}H_{40}N_4$, 768.3253; found, 768.3251. Anal. calcd. for $C_{56}H_{40}N_4$: C 87.47, H 5.24, N 7.29; found: C 87.43, H 5.28, N 7.27.

DOI: 10.1002/adma.201202222

CCDC-872027 and CCDC-872028 contain the supplementary crystallographic data for this paper. These data can be obtained free of charge from The Cambridge Crystallographic Data Centre via www.ccdc.cam.ac.uk/data_request/cif.

Supporting Information

Supporting Information is available from the Wiley Online Library or from the author.

Acknowledgements

We thank the Ministry of Economic Affairs (100-EC-17-A-08-S1-042) and the National Science Council (NSC-100-2119-M-007-010-MY3) for support of this research and the National Center for High-Performance Computing (Account number: u32chc04) of Taiwan for providing the computing time.

Received: June 2, 2012
Revised: July 23, 2012
Published online:

---

[1] a) C. W. Tang, S. A. Vanslyke, *Appl. Phys. Lett.* **1987**, *51*, 913; b) C. C. Wu, Y. T. Lin, K. T. Wong, R. T. Chen, Y. Y. Chien, *Adv. Mater.* **2004**, *16*, 61; c) M. T. Lee, C. H. Liao, C. H. Tsai, C. H. Chen, *Adv. Mater.* **2005**, *17*, 2493; d) H. B. Wu, L. Ying, W. Yang, Y. Cao, *Chem. Soc. Rev.* **2009**, *38*, 3391; e) M. A. Baldo, M. E. Thompson, S. R. Forrest, *Nature* **2000**, *403*, 750; f) J. Kido, M. Kimura, K. Nagai, *Science* **1995**, *267*, 1332.

[2] K. C. Wu, P. J. Ku, C. S. Lin, H. T. Shih, F. I. Wu, M. J. Huang, J. J. Lin, I. C. Chen, C. H. Cheng, *Adv. Funct. Mater.* **2008**, *18*, 67.

[3] H. H. Chou, C. H. Cheng, *Adv. Mater.* **2010**, *22*, 2468.

[4] S.-J. Su, H. Sasabe, T. Takeda, J. Kido, *Chem. Mater.* **2008**, *20*, 1691.

[5] C. W. Tang, S. A. Van Slyke, C. H. Chen, *J. Appl. Phys.* **1989**, *65*, 3610.

[6] M. T. Lee, H. H. Chen, C. H. Liao, C. H. Tsai, C. H. Chen, *Appl. Phys. Lett.* **2004**, *85*, 3301.

[7] C. Hosokawa, H. Higashi, H. Nakamura, T. Kusumoto, *Appl. Phys. Lett.* **1995**, *67*, 3853.

[8] H. Higashi, C. Hosokawa, H. Tokailin, T. Kusumoto, *Nippon Kagaku Kaishi* **1992**, *10*, 1162.

[9] a) J. H. Lee, T. C. Lin, C. C. Liao, *Proc. SPIE* **2005**, *5740*, 138; b) Y. H. Ho, T. C. Lin, C. F. Wu, J. H. Lee, *Proc. SPIE* **2006**, *6333*, 633303.

[10] S. J. Lee, J. S. Park, K.-J. Yoon, Y.-I. Kim, S.-H. Jin, S. K. Kang, Y.-S. Gal, S. Kang, J. Y. Lee, J.-W. Kang, S.-H. Lee, H.-D. Park, J.-J. Kim, *Adv. Funct. Mater.* **2008**, *18*, 3922.

[11] a) K. H. Lee, L. K. Kang, J. Y. Lee, S. Kang, S. O. Jeon, K. S. Yook, J. Y. Lee, *Adv. Funct. Mater.* **2010**, *20*, 1345; b) K. H. Lee, C. S. Son, J. Y. Lee, S. Kang, K. S. Yook, S. O. Jeon, J. Y. Lee, S. S. Yoon, *Eur. J. Org. Chem.* **2011**, *25*, 4788; c) K. H. Lee, Y. S. Kwon, J. Y. Lee, S. Kang, K. S. Yook, S. O. Jeon, J. Y. Lee, S. S. Yoon, *Chem. Eur. J.* **2011**, *17*, 12994.

[12] Y.-H. Chen, H.-H. Chou, T.-H. Su, P.-Y. Chou, F.-I. Wu, C.-H. Cheng, *Chem. Commun.* **2011**, *47*, 8865.

[13] a) K. Suzuki, A. Seno, H. Tanabe, K. Ueno, *Synth. Met.* **2004**, *143*, 89; b) K. R. Wee, H. C. Ahn, H. J. Son, W. S. Han, J. E. Kim, D. W. Cho, S. O. Kang, *J. Org. Chem.* **2009**, *74*, 8472; c) Y. S. Kwon, K. H. Lee, G. Y. Kim, J. H. Seo, Y. K. Kim, S. S. Yoon, *J. Nanosci. Nanotechnol.* **2009**, *9*, 7056; d) K. H. Lee, Y. S. Kwon, L. K. Kang, G. Y. Kim, J. H. Seo, Y. K. Kim, S. S. Yoon, *Synth. Met.* **2009**, *159*, 2603.

[14] a) K. Tamao, M. Uchida, T. Izumizawa, K. Furukawa, S. Yamaguchi, *J. Am. Chem. Soc.* **1996**, *118*, 11974; b) J. Shi, W. Tang, C. H. Chen, *US Patent 5646948*, **1997**; c) Z. Wang, P. Lu, S. Chen, Z. Gao, F. Shen, W. Zhang, Y. Xu, H. S. Kwok, Y. Ma, *J. Mater. Chem.* **2011**, *21*, 5451; d) A. P. Kulkarni, C. J. Tonzola, A. Babel, S. A. Jenekhe, *Chem. Mater.* **2004**, *16*, 4556.

[15] a) Z. Ge, T. Hayakawa, S. Ando, M. Ueda, T. Akiike, H. Miyamoto, T. Kajita, M. Kakimoto, *Chem. Mater.* **2008**, *20*, 2532; b) S. Takizawa, V. A. Montes, P. Anzenbacher Jr., *Chem. Mater.* **2009**, *21*, 2452; c) W.-Y. Hung, L.-C. Chi, W.-J. Chen, Y.-M. Chen, S.-H. Chou, K.-T. Wong, *J. Mater. Chem.* **2010**, *20*, 10113; d) S. Gong, Y. Chen, C. Yang, C. Zhong, J. Qin, D. Ma, *Adv. Mater.* **2010**, *22*, 5370; e) S. Gong, Y. Chen, J. Luo, C. Yang, C. Zhong, J. Qin, D. Ma, *Adv. Funct. Mater.* **2011**, *21*, 1168; f) Y.-M. Chen, W.-Y. Hung, H.-W. You, A. Chaskar, H.-C. Ting, H.-F. Chen, K.-T. Wong, Y.-H. Liu, *J. Mater. Chem.* **2011**, *21*, 14971.

[16] A. Islam, C.-C. Tsou, H.-J. Hsu, W.-L. Shih, C.-H. Liu, C.-H. Cheng, *Tamkang J.Sci. Eng.* **2002**, *5*, 69.

[17] C.-H. Chen, F.-I. Wu, C.-F. Shu, C.-H. Chien, Y.-T. Tao, *J. Mater. Chem.* **2004**, *14*, 1585.

[18] a) C. J. Kuo, T. Y. Li, C. C. Lien, C. H. Liu, F. I. Wu, M. J. Huang, *J. Mater. Chem.* **2009**, *19*, 1865; b) V. K. Mahesh, M. Maheswari, R. Sharma, *Can. J. Chem.* **1985**, *63*, 635.

[19] The supplementary crystallographic data of PPIE and TPIE are listed in CCDC-872027 and CCDC-872028, respectively. These data can be obtained free of charge from The Cambridge Crystallographic Data Centre via www.ccdc.cam.ac.uk/data_request/cif.

[20] K.-C. Wu, P.-J. Ku, C.-S. Lin, H.-T. Shih, F.-I. Wu, M.-J. Huang, J.-J. Lin, I.-C. Chen, C.-H. Cheng, *Adv. Funct. Mater.* **2008**, *18*, 67.

[21] Y. Li, J. Ding, M. Day, Y. Tao, J. Lu, M. D'iorio, *Chem. Mater.* **2004**, *16*, 2165.